Dalton Transactions

Accepted Manuscript

ROYAL SOCIETY OF CHEMISTRY

www.rsc.org/dalton

Cite this: DOI: 10.1039/c0xx00000x

www.rsc.org/xxxxxx

ARTICLE TYPE

Synthesis and physical properties of layered Ba_xCoO_2

Jinfeng Liu[a], Xiangyang Huang*[b], Danfeng Yang[a], Guisheng Xu[a] and Lidong Chen[b]

Received (in XXX, XXX) Xth XXXXXXXXX 20XX, Accepted Xth XXXXXXXXX 20XX
DOI: 10.1039/b000000x

Abstract

A layered cobaltite Ba_xCoO_2 (x = 0.19, 0.28, 0.30, 0.33) has been synthesized by an ion exchange technique from the layered Na_xCoO_2 precursors. The phase composition and physical properties were investigated. Ba_xCoO_2 is isomorphic to the precursor Na_xCoO_2. The magnetic susceptibility of Ba_xCoO_2 decreases with increasing the barium content and shows a Curie-Weiss-like behavior at temperatures above 50 K. The resistivity is sensitive to the barium content. As the barium content increases from 0.19 to 0.33, a crossover from a semiconducting behavior to a metallic behavior was observed. The Seebeck coefficient of Ba_xCoO_2 is insensitive to the barium content due to the tradeoff effect between the carrier concentration and Co^{4+} content, while the thermal conductivity increases with increasing the barium content from 0.19 to 0.33 owing to the ordered state of Ba ions between the CoO_2 layers.

1. Introduction

Since the $Na_{0.50}CoO_2$ single crystal was discovered to exhibit a large Seebeck coefficient as well as a low resistivity in 1997[1], misfit cobaltites have been considered to be one of the potential candidates for thermoelectric applications. The crystal structure of those cobaltites, such as Na_xCoO_2[1], $[Sr_2O_2]_qCoO_2$[2], $Ca_3Co_4O_9$[3], $Bi_2Sr_2Co_2O_9$[4], contain the hexagonal CdI_2-type CoO_2 layers and the single, double, triple, or quadruple layered blocks, which are alternately stacked along the c axis. It was generally supposed that the CdI_2-type CoO_2 layer along with the natural superlattice structure feature in the layered cobaltites play a very important role in the thermoelectric properties[5].

In recent years, some other new layered cobaltites, Ca_xCoO_2[6], Sr_xCoO_2[7, 8], and Ln_xCoO_2(Ln = La, Pr, and Nd)[9, 10] synthesized by an ion exchange technique from the Na_xCoO_2 precursor[11,12] have been reported to exhibit a large Seebeck coefficient, low resistivity or low thermal conductivity, which are necessary for a good thermoelectric material with high ZT value ($ZT = S^2\sigma T/\kappa$, where S, σ, κ, T are the Seebeck coefficient, electrical conductivity, thermal conductivity, and absolute temperature, respectively). For $Ca_{0.33}CoO_2$ crystal, the resistivity and Seebeck coefficient in ab-plane is 0.74 mΩ cm and 81 μV/K at 300 K, respectively, and the power factor is about 25% higher than that of the $Ca_3Co_4O_9$ crystal[6]. For $Sr_{0.29}CoO_2$ crystal, the resistivity and Seebeck coefficient in ab-plane at 300 K is 2 mΩ cm and 78 μV/K, respectively[8], and for $Sr_{0.29}CoO_2$ polycrystalline, the resistivity and Seebeck coefficient is 9 mΩ cm and 70 μV/K at 300 K[7]. However, for Ln_xCoO_2 polycrystalline, although the Seebeck coefficient at room temperature is over 175 μV/K and the thermal conductivity is as low as 1 W m^{-1} K^{-1}, the resistivity is about 10^4 mΩ cm, four order of magnitude higher than that of alkaline earth cobaltites. More importantly, in the ion exchange reaction of synthesizing Ca_xCoO_2[11], Sr_xCoO_2[7], and Ln_xCoO_2[9, 10], only the Na^+ ions were substituted by the Ca^{2+}, Sr^{2+}or Ln^{3+} ions, while the CdI_2-type CoO_2 layers still maintained the hexagonal CdI_2-type structure, resulting in the exchange products being isostructural to their precursor Na_xCoO_2 with a layered structure[6, 7, 9]. Those results indicate that the ion exchange reaction can provide an important route to synthesize new layered cobaltites, which may have good thermoelectric properties.

T. Kajitani *et al.* has ever prepared $Ba_{0.35}CoO_2$ by solid-state reaction using $Na_{0.70}CoO_2$ and $Ba(NO_3)_2$[13]. The X-ray diffraction results showed that $Ba_{0.35}CoO_2$ was isostructural to the precursor $Na_{0.70}CoO_2$. However, no detailed study on the physical properties of Ba_xCoO_2 has been reported. In this contribution, we report the synthesis of layered Ba_xCoO_2 by another method-ion exchange reaction in flux, and the magnetization and thermoelectric properties.

2. Experimental details

Polycrystalline samples of Ba_xCoO_2 were synthesized through the low temperature ion exchange technique from Na_xCoO_2 precursors, and the polycrystalline precursors, Na_xCoO_2, with the nominal composition of x = 0.70, 0.80 and 0.90 were prepared by a conventional solid state reaction. A stoichiometric amount of reagent grade Na_2CO_3 and Co_3O_4 was mixed and calcined at 850 °C for 20 h in air, and then reground and calcined at 850 °C for another 20 h. Since sodium tends to evaporate during calcination, the actual content of sodium in Na_xCoO_2 was lower than the nominal composition. A lower sodium concentration Na_xCoO_2 sample was prepared by chemically de-intercalating sodium from Na_xCoO_2 (x = 0.7) using bromine as an oxidizing agent, similar to that described in ref. 14. The ion exchange was carried out by reacting Na_xCoO_2 with molten $Ba(NO_3)_2$ and KNO_3 at 500 °C for 50 h. The molar ratio of $Ba(NO_3)_2$ to KNO_3 was 1:1. After the reaction, the ion exchange products were collected, washed with distilled water and dried at 120 °C in air. Finally, the powder samples were consolidated by spark plasma sintering (SPS) at 400°C for 5 min under a pressure of 300 MPa.

The crystal structure and chemical composition of the samples were determined by powder x-ray diffraction (XRD) analysis (Cu K_α, Rigaku, Rint2000) and inductively coupled plasma atomic

emission spectroscopy (ICP-AES) measurement (Agilent, 710), respectively. The low temperature magnetic susceptibility (χ), electrical resistivity (ρ), Seebeck coefficient (S), thermal conductivity (κ) and Hall coefficient (R_H) were measured using a physical property measurement system (PPMS, Quantum Design).

3. Results and discussion

Table I. ICP-AES results of Ba_xCoO_2.

Ba_xCoO_2	Ba : Co : Na (atom ratio)	Ba (mass percent %)	Co (mass percent %)	Na (mass percent %)
$Ba_{0.19}CoO_2$	0.19 : 1.00 : 0.0017	24.42	54.11	0.040
$Ba_{0.28}CoO_2$	0.28 : 1.00 : 0.0023	30.42	46.49	0.054
$Ba_{0.30}CoO_2$	0.30 : 1.00 : 0.0020	32.58	46.53	0.047
$Ba_{0.33}CoO_2$	0.33 : 1.00 : 0.0019	35.39	46.04	0.043

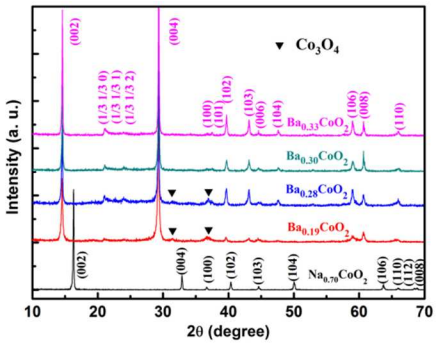

Fig. 1. Powder XRD patterns for Ba_xCoO_2(x = 0.19, 0.28, 0.30, 0.33) and one of the precursor $Na_{0.70}CoO_2$.

The actual Ba contents in Ba_xCoO_2 were determined by ICP-AES, and listed in Table I. Only trace amount of sodium was detected in the ion exchange products and can be neglected. The samples Ba_xCoO_2 (x = 0.28, 0.30, 0.33) were the ion exchange resultants of γ-Na_yCoO_2 (y = 0.7, 0.8, 0.9, nominal composition), respectively. The precursor of $Ba_{0.19}CoO_2$ was prepared by chemically de-intercalating sodium from $Na_{0.7}CoO_2$ using bromine as an oxidizing agent. The XRD patterns of one of the precursor γ-$Na_{0.70}CoO_2$ and the ion exchange products Ba_xCoO_2 (x = 0.19, 0.28, 0.30, 0.33) are shown in Fig. 1. A strong correlation exists between the structure of γ-$Na_{0.70}CoO_2$ and Ba_xCoO_2, which was expected from the topotactic nature of the ion exchange reactions[11]. The patterns could be indexed on a hexagonal unit cell with the space group of $P6_3/mmc$, which agrees with the previous structural analysis of the ion exchange resultants Ca_xCoO_2[12], Sr_xCoO_2[7], and La_xCoO_2[9]. The XRD results indicate that the ion exchange resultants Ba_xCoO_2 are isostructural to the precursors γ-Na_xCoO_2. Compared to the peaks of the precursor γ-$Na_{0.70}CoO_2$, the (hkl) peaks ($l \neq 0$) of Ba_xCoO_2 shift toward lower 2θ range, while the (hk0) peaks, such as (100) and (110), did not shift much. Since only the larger Ba^{2+} ions substitute the smaller Na^+ ions in the single block layer between the CoO_2 layers and the CoO_2 layers still maintain the hexagonal CdI_2-type structure. As a result, the lattice parameter c would become larger as indicated in the following Figure 2, while the lattice parameters a and b did not change much (not shown here). For the $Ba_{0.19}CoO_2$ and $Ba_{0.28}CoO_2$ samples, some weak diffraction peaks from a tiny trace of Co_3O_4 impurity were observed, marked by triangles in the Fig. 1. In addition, some highly asymmetric extra peaks were detected in the 2θ range from 20° to 25°. They show a sharp edge from the low 2θ side and a long tail at the high 2θ, which is similar to the XRD results of Sr_xCoO_2[7] and La_xCoO_2[9], and caused by the superstructure[9].

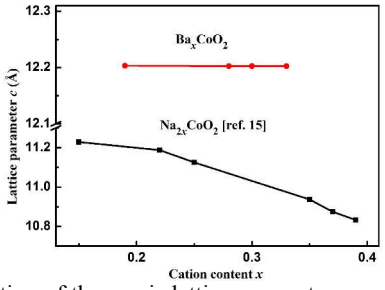

Fig. 2. Variation of the c-axis lattice parameter c as a function of cation content x.

Fig. 2 shows the c-axis lattice parameters of Ba_xCoO_2 and Na_xCoO_2 as a function of the cation content. The c-axis lattice parameters of Na_xCoO_2 were taken from ref. 15. The lattice parameter c of Ba_xCoO_2 is almost unchanged with Ba ions content x, which is different from the Na_xCoO_2 precursors. This suggests that the stronger electrostatic interaction between the Ba^{2+} ions and O^{2-} ions is enough to overcome the repulsion between the negatively charged layers. A similar relationship between the CoO_2 layer-spacing and the composition in Ca_xCoO_2[6] and Sr_xCoO_2[15] was also observed.

Table II. Curie-Wiess fitting parameters of Ba_xCoO_2.

samples	χ_0(×10^{-3}) [emu/(molOe)]	C (×10^{-3}) [emu K/(molOe)]	Θ (K)	M_{eff} μ_B/Co
$Ba_{0.19}CoO2$	0.20	482.04	-68.44	1.96
$Ba_{0.28}CoO2$	0.10	425.31	-93.89	1.84
$Ba_{0.30}CoO2$	0.14	301.1	-102.93	1.55
$Ba_{0.33}CoO2$	0.12	266.61	-115.24	1.46

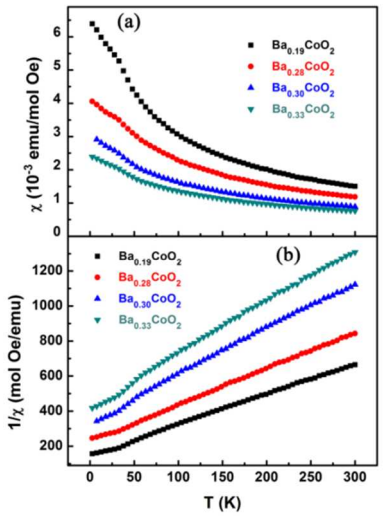

Fig. 3. Temperature dependence of the magnetic susceptibility χ and inverse susceptibility 1/χ for Ba_xCoO_2 in a field of 5 T.

Fig. 3 is the temperature dependences of χ and inverse χ for the Ba_xCoO_2 samples, measured in a field of 5 T. The χ value of the four samples increased with decreasing temperature and showed a Curie-Weiss-like behavior at temperatures above 50 K, while a

deviation was noticed at temperatures below 50 K, indicating an increase of the magnetic interaction. The χ value for Ba_xCoO_2 decreased with increasing the Ba content, implying a decrease of the magnetic moments. Above 50 K, the χ value can be analyzed by the Curie-Weiss law with the formula $\chi = C/(T-\Theta) + \chi_0$, where C, Θ and χ_0 are the Curie constant, Weiss temperature and temperature independent term, respectively. The fitting parameters are shown in Table II. The effective moments M_{eff} of Co ions were determined from the Curie Constant C. In Ba_xCoO_2, Co^{3+} and Co^{4+} coexist as in Na_xCoO_2[16]. The occupancy of Co^{4+} increases with decreasing x owing to a fraction (1-2x) of Co ions being in the Co^{4+} state. The Curie-Weiss behavior in χ was considered to be induced by magnetic Co^{4+} ions. Consequently, the M_{eff} of Ba_xCoO_2 decrease with increasing x, due to the decreasing concentration of Co^{4+} ions. On the other hand, the temperature dependence of χ of Ba_xCoO_2 with the cation concentration was found to be different from that of Na_xCoO_2[17], but similar with that of Sr_xCoO_2[15]. The χ value of Na_xCoO_2 changes from a Curie-Weiss-like behavior for $x > 0.5$ to a relatively T-dependent Pauli paramagnetic behavior for $x < 0.5$[17], while the χ value of Ba_xCoO_2 and Sr_xCoO_2 still shows a Curie-Weiss-like behavior even at the low cation content.

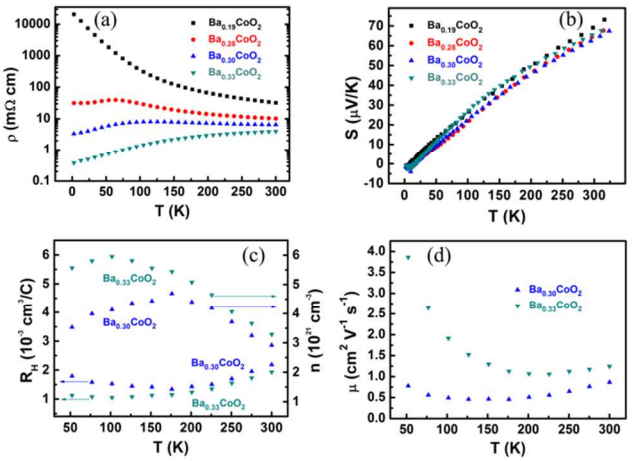

Fig. 4. Temperature dependence of (a) resistivity ρ, (b) Seebeck coefficient S, (c) Hall coefficient R_H and carrier concentration n, and (d) mobility μ for Ba_xCoO_2 at temperatures below 300 K.

Fig. 4(a) displays the temperature dependence of ρ for Ba_xCoO_2. With increasing x from 0.19 to 0.33, the magnitude of ρ decreased dramatically, and the ρ value for Ba_xCoO_2(x = 0.19, 0.28, 0.30, 0.33) at 300 K was 32.4 mΩ cm, 10.2 mΩ cm, 6.5 mΩ cm, and 4.0 mΩ cm, respectively, which implies that ρ was very sensitive to the barium content. The ρ of $Ba_{0.33}CoO_2$ is the lowest in the four samples, which is similar to the results of Sr_xCoO_2 reported by Y. G. Guo *et al.*[15]. The ρ of $Sr_{0.35}CoO_2$ is lower than the other five samples, for which the content of strontium is 0.15, 0.22, 0.25, 0.37 and 0.39. A crossover from a semiconducting behavior to a metallic behavior was observed with increasing barium content from 0.19 to 0.33. $Ba_{0.19}CoO_2$ exhibits a semiconducting behavior, and $Ba_{0.33}CoO_2$ exhibits a metallic behavior in the whole measured temperature range. However, for $Ba_{0.28}CoO_2$ and $Ba_{0.30}CoO_2$, the resistivity is metallic at low temperatures, but exhibits a semiconducting behavior at high temperatures. The difference in ρ of Ba_xCoO_2 should be attributed to the difference in carrier density n along with carrier mobility μ.

As discussed later in Seebeck coefficient part, Ba_xCoO_2 showed the p-type behavior and the carrier was hole. Fig. 4(c) presents the temperature dependence of R_H and n ($n = 1/eR_H$) for $Ba_{0.30}CoO_2$ and $Ba_{0.33}CoO_2$. The n for $Ba_{0.33}CoO_2$ was higher than that for $Ba_{0.30}CoO_2$, which is owing to the well-defined Ba-ordered state appears at $x \approx 1/3$ as Ca_xCoO_2[18], Sr_xCoO_2[19, 20], and La_xCoO_2[9]. The barium ions between the CoO_2 layers deviated the ordered state when the concentration of the barium was less than 1/3 or more than 1/3. Due to the reduction of n, the average distance between the hole carriers increased, which could lead to the increase in the localization of holes[21]. Consequently, μ ($\mu = R_H/\rho$) of the system (shown in Fig. 4(d)) also decreased with decreasing barium content, and the difference of μ was enlarged with decreasing temperature. Furthermore, in such a strongly correlated system, the increase of the average distance between the carriers would enhance electronic correlations and cause the decrease of the bandwidth[15, 21]. Accordingly, as the bandwidth narrows, the system will change from a metallic behavior to a semiconducting behavior.

The n of the two samples increased with decreasing temperature first, which is commonly seen in the layered cobalt oxides[8, 22]. And then, a drop is observed about 175 K and 100 K for $Ba_{0.30}CoO_2$ and $Ba_{0.33}CoO_2$, respectively. We assume that this is related to the coexistence of two Fermi surfaces of different natures, which is similar to its precursor Na_xCoO_2 and predicted by the calculation of the band structure of $Na_{0.5}CoO_2$[23]. One is the narrow a_{1g} band providing localized carriers, and the other is the wide a_{1g}+e_g band providing itinerant carriers. As the temperature decreasing, the Fermi surface for the lower mobility carriers vanishes upon a carrier localization effect, so the n of the two samples decreased with decreasing temperature at low temperatures. On the other hand, the Fermi surface for the higher mobility carriers still survives. Thus, the ρ still decreased with decreasing temperature, because ρ is inversely proportional to the total scattering time average over the whole Fermi surface[8, 22].

Fig. 4(b) shows the temperature dependence of S for Ba_xCoO_2. All the four samples present similar S behavior. As the barium content increases, the S for Ba_xCoO_2(x = 0.19, 0.28, 0.30, 0.33) at 300 K is 70 μV/K, 65 μV/K, 64 μV/K, and 65 μV/K, respectively. Namely, S was insensitive to the barium content. In Ba_xCoO_2, not only the carrier density but also the concentration of the Co^{4+} ions is very important for S. In general, S can be expressed using the Mott formula (originating from the Sommerfeld expansion)[24].

$$S = \frac{\pi^2 \kappa_B^2 T}{3e}\left[\frac{\partial \ln \sigma(\varepsilon)}{\partial \varepsilon}\right]_{\varepsilon=\varepsilon_F} \qquad (1)$$

By substituting $\sigma = en\mu(\varepsilon)$ in formula (1), we can obtain

$$S = \frac{C_e}{n} + \frac{\pi^2 \kappa_B^2 T}{3e}\left[\frac{\partial \ln \mu(\varepsilon)}{\partial \varepsilon}\right]_{\varepsilon=\varepsilon_F} \qquad (2)$$

Where C_e, n, $\mu(\varepsilon)$, and κ_B are the specific heat, carrier concentration, energy correlated carrier mobility, and Boltzmann constant, respectively. The first term of Eq. (2) is dominant, so the change in S can usually be explained by the alteration of carrier concentration n. Therefore, according to Eq. (2), the S of

Ba_xCoO_2 increases with decreasing n, which decreases with decreasing barium content. However, for the layered cobaltites, the S value can also be expressed by the following formula:[25]

$$S = -\frac{\kappa_B}{e} ln\left(\frac{g_3}{g_4}\frac{x}{1-x}\right) \quad (3)$$

where κ_B, g_3, g_4 and x are the Boltzmann constant, numbers of the spin configuration of Co^{3+} and Co^{4+} and concentration of Co^{4+} ions, respectively. In Ca_xCoO_2 and Sr_xCoO_2, the $Co^{3+}$and Co^{4+} are in low-spin state[6, 8, 25], so the $Co^{3+}$and Co^{4+} in Ba_xCoO_2 may also be in low-spin state. Therefore, g_3/g_4 =1/6, and according to Eq. (3), the S value of Ba_xCoO_2 decreases with increasing the concentration of Co^{4+} ions, which increases with decreasing barium content. As a result, the S value of Ba_xCoO_2 was the tradeoff results of these two factors and therefore not sensitive to the barium content.

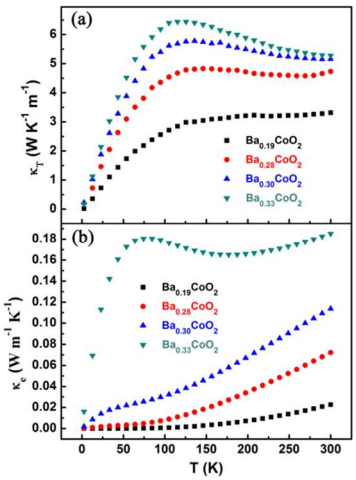

Fig. 5. Temperature dependence of the total thermal conductivity κ_T and carrier thermal conductivity κ_e for Ba_xCoO_2 at temperatures below 300 K.

The total thermal conductivity of a solid can be written as $\kappa_T = \kappa_L + \kappa_e$, where κ_T, κ_L and κ_e are the total, lattice and carrier thermal conductivities, respectively. The value of κ_e can be estimated from Wiedemann-Franz law, $\kappa_e = LT/\rho$, where L is the Lorentz number (2.45×10^{-8} V^2 K^{-2} for free electrons). Fig. 5(a) and (b) present the temperature dependence of κ_T and κ_e for Ba_xCoO_2, respectively. The κ_e value was much lower than the κ_T value, indicating that κ_T was dominated by the lattice component in the Ba_xCoO_2 samples. κ_T increased with the increase of barium content from 0.19 to 0.33. We speculate this is also related to the ordered state of barium between the CoO_2 layers. As indicated before, for the $Ba_{0.33}CoO_2$ sample, the barium ions in the CoO_2 layers were in the ordered state, and could not strongly scatter the phonon, while for the other three samples, the barium ions deviated the ordered state more or less, and the lower the barium content was, the stronger the barium ions scattered the phonon, and thus the lower the κ_T value was.

4. Conclusions

In summary, polycrystalline samples of Ba_xCoO_2 (x = 0.19, 0.28, 0.30, 0.33) have been successfully fabricated by an ion exchange technique. The Ba_xCoO_2 compounds are isostructural to γ-Na_xCoO_2 with a layered hexagonal structure. The magnetic susceptibility of all the four samples shows a Curie-Weiss-like behavior at temperatures above 50 K, and the effective magnetic moments decrease with increasing barium content. Different resistivity behavior was observed for Ba_xCoO_2 with varying x, and the resistivity undergoes a semiconducting to a metallic crossover with increasing barium content from 0.19 to 0.33 due to the change of the bandwidth. Since the effects of carrier concentration and Co^{4+} concentration cancelled out, the Seebeck coefficient of Ba_xCoO_2 is insensitive to the barium content. Owing to the ordered state of barium between the CoO_2 layers, the thermal conductivity increases with increasing the barium content from 0.19 to 0.33.

[a] *Key Laboratory of Transparent Opto-Functional Advanced Inorganic Materials, Shanghai Institute of Ceramics, Chinese Academy of Sciences, 1295 Dingxi Road, Shanghai 200050, P. R. China. Fax: +86 21 52927184; Tel: +86 21 69987754*

[b] *CAS Key Laboratory of Materials for Energy Conversion, Shanghai Institute of Ceramics, Chinese Academy of Sciences, 1295 Dingxi Road, Shanghai 200050, P.R. China. Fax: +86 21 69987781; Tel: +86 21 69987721*

Reference

1 I. Terasaki, Y. Sasago and K. Uchinokura, *Phys. Rev. B*, 1997, **56**, 12685.
2 H. Yamauchi, K. Sakai, T. Nagai, Y. Matsui and M. Karppinen, *Chem. Mater.*, 2006, **18**, 155.
3 A. C. Masset, C. Michel, A. Maignan, H. Hervieu, O. Toulemonde, F. Studer, B. Raveau and J. Hejtmanek, *Phys. Rev. B*, 2000, **62**, 166.
4 R. Funahashi and I. Matsubara, *Appl. Phys. Lett.*, 2001, **79**, 362.
5 I. Terasaki, M. Iwakawa, T. Nakano, A. Tsukuda and W. Kobayashi, *Dalton Trans.*, 2010, **39**, 1005.
6 J. F. Liu, X. Y. Huang, F. Li, R. H. Liu and L. D. Chen, *J. Phys. Soc. Jpn.*, 2011, **80**, 074802.
7 R. Ishikawa, Y. Ono, Y. Miyazaki and T. Kajitani, *Jpn. J. Appl. Phys.*, 2002, **41**, 337.
8 J. F. Liu, X. Y. Huang, G. S. Xu and L. D. Chen, *J. Alloys Comp.*, 2013, **576**, 247.
9 K. Knížek, J. Hejtmánek, M. Maryško, E. Šantavá, Z. Jirák, J. Buršík, K. Kirakci and P. Beran, *J. Solid State Chem.*, 2011, **184**, 2231.
10 K. Knížek, Z. Jirák, J. Hejtmánek, M. Maryško and J. Buršík, *J. Appl. Phys.*, 2012, **111**, 07D707.
11 B. L. Cushing, A. U. Falster, W. B. Simmons and J. B. Wiley, *Chem. Commun.*, 1996, **23**, 2635.
12 B. L. Cushing and J. B. Wiley, *J. Solid State Chem.*, 1998, **141**, 385.
13 T. Kajitani, Y. Ono, Y. Miyazaki and Y. Morii, *21st International Conference on Thermoelectrics*, 2002, 195.
14 R. E. Schaak, T. Klimczuk, M. L. Foo and R. J. Cava, *Nature*, 2003, **424**, 527.
15 Y. G. Guo, J. L. Luo, G. T. Liu, H. Y. Yang, J. Q. Li, N. L. Wang and D. Jin, *Phys. Rev. B*, 2006, **74**, 155129.
16 D. Wu, J. L. Luo and N. L. Wang, *Phys. Rev. B*, 2006, **73**, 014523.
17 M. L. Foo, Y. Wang, S. Watauchi, H. W. Zandbergen, T. He, R. J. Cava and N. P. Ong, *Phys. Rev. Lett.*, 2004, **92**, 247001.
18 H. Y. Yang, Y. G. Shi, X. Liu, R. J. Xiao, H. F. Tian and J. Q. Li, *Phys. Rev. B*, 2006, **73**, 014109.
19 H. Y. Yang, Y. G. Shi, Y. G. Guo, X. Liu, R. J. Xiao, J. L. Luo and J. Q. Li, *Mater. Res. Bull.*, 2007, **42**, 94.
20 L. D. Yao, Y. G. Guo, J. L. Luo, W. Zhang, F. Y. Li, C. Q. Jin and R. C. Yu, *Phys. Rev. B*, 2007, **75**, 174118.
21 Y. Wang, Y. Shi, J. G. Cheng, X. J. Wang, W. H. Su, X. Y. Liu and H. J. Fan, *J. Phys. Chem.* C, 2010, **114**, 5174.
22 M. Mikami, M. Yoshimura, Y. Mori, T. Sasaki, R. Funahashi, and M. Shikano, *Jpn. J. Appl. Phys.*2003, **42**, 7383.
23 D. J. Singh, *Phys. Rev. B* 2000, **61**, 13397.
24 B. Fisher, L. Patlagan, G. M. Reisner and A. Knizhnik, *Phys. Rev. B*, 2000, **61**, 470.

25 W. Koshibae, K. Tsutsui and S. Maekawa, *Phys. Rev. B*, 2000, **62**, 6869.